Anesthesia-induced loss of consciousness disrupts auditory responses beyond primary cortex

Aaron J Krom[1,2,§], Amit Marmelshtein[3,§], Hagar Gelbard-Sagiv[2], Ariel Tankus[3,4,5], Daniel Hayat[6], Idit Matot[6], Ido Strauss[4], Firas Fahoum[7], Martin Soehle[8], Jan Boström[9], Florian Mormann[10], Itzhak Fried[4,11] and Yuval Nir[2,3*]

[1] Department of Anesthesiology and Critical Care Medicine, Hadassah-Hebrew University Medical Center, Hebrew University-Hadassah School of Medicine, Jerusalem, Israel
[2] Department of Physiology & Pharmacology, Sackler School of Medicine, Tel Aviv University, Israel
[3] Sagol School of Neuroscience, Tel Aviv University, Israel
[4] Functional Neurosurgery Unit, Tel Aviv Sourasky Medical Center, Tel Aviv, Israel
[5] Department of Neurology & Neurosurgery, Sackler School of Medicine, Tel Aviv University, Israel
[6] Department of Anesthesia, Intensive Care and Pain, Tel Aviv Medical Center, Sackler Medical School, Tel Aviv University, Tel Aviv, Israel
[7] EEG and Epilepsy Unit, Department of Neurology, Tel Aviv Sourasky Medical Center, Tel Aviv, Israel
[8] Department of Anesthesiology; University of Bonn, Germany
[9] Department of Neurosurgery; University of Bonn, Germany
[10] Department of Epileptology; University of Bonn, Germany
[11] Department of Neurosurgery, University of California Los Angeles, Los Angeles, USA

§ Equal contribution
* Corresponding author and lead contact

Keywords

propofol, human, single-unit, LFP, gamma power

Abstract

Despite its ubiquitous use in medicine, and extensive knowledge of its molecular and cellular effects, how anesthesia induces loss of consciousness (LOC) and affects sensory processing remains poorly understood. Specifically, it is unclear whether anesthesia primarily disrupts thalamocortical relay or intercortical signaling. Here we recorded intracranial EEG (iEEG), local field potentials (LFPs), and single-unit activity in patients during wakefulness and light anesthesia. Propofol infusion was gradually increased while auditory stimuli were presented and patients responded to a target stimulus until they became unresponsive. We found widespread iEEG responses in association cortices during wakefulness, which were attenuated and restricted to auditory regions upon LOC. Neuronal spiking and LFP responses in primary auditory cortex (PAC) persisted after LOC, while responses in higher-order auditory regions were variable, with neuronal spiking largely attenuated. Gamma power induced by word stimuli increased after LOC while its frequency profile slowed, decoupling from local spiking activity. In summary, anesthesia-induced LOC disrupts auditory processing in association cortices while relatively sparing responses in PAC.

2

Introduction

The practice of administering general anesthesia, which began over 170 years ago, revolutionized medicine by transforming surgery from being a deeply traumatic experience into a humane therapy[1,2] and enabling complex procedures to be performed. In the US, nearly 60,000 patients per day undergo general anesthesia[3]: a drug-induced, reversible condition that includes unconsciousness, amnesia, analgesia, and akinesia. By now, we have extensive knowledge of the molecular and cellular effects of anesthetics[4–7]; but how anesthetic drugs induce loss of consciousness remains a central unresolved question in medicine[8]. Given that anesthetics act at diverse molecular and cellular targets[7,9], their effects on consciousness and sensory perception are best studied at the level of common brain circuits and systems[2,9,10].

Traditionally, sensory pathways were studied in anesthetized animals where robust responses in primary sensory regions prompted seminal discoveries on the organizational principles in multiple modalities[11–13]. With time, research expanded to awake animals and a number of studies directly compared sensory processing across wakefulness and anesthesia, revealing state-dependent evoked responses in the visual[14–16] and somatosensory domains[17,18]. However, these modalities heavily depend on active sensing (i.e. eye movements, whisking)[19] and its absence in anesthesia limits interpretation as reflecting LOC.

In the auditory domain where processing is largely passive, anesthesia was originally reported to reduce responses in auditory cortex[20–22], but recent studies with light anesthesia challenge this view[23]. In humans, effects of anesthesia have been reported for mid-latency cortical evoked potentials[24] and for high-frequency (40Hz) steady-state potentials[25]. Functional magnetic resonance imaging (fMRI) studies revealed differential responses across wakefulness and anesthesia[26–28], but interpretation is limited by poor temporal resolution

and by relying on hemodynamics that change upon anesthesia[29]. Generally, previous studies that compared sensory processing across wakefulness and anesthesia mostly focused on activity up to primary sensory cortex[20–22], often employed deep anesthesia at surgical levels[25,28], entailed uncertainty about the precise moment of LOC in animal models, or relied on non-invasive measures in humans with limited resolution[25–28,30]. We sought to go beyond these limitations to better understand how anesthesia-induced LOC affects sensory processing. In particular, we aimed to address a central unresolved question in the field: whether anesthesia-induced LOC primarily affects bottom-up thalamocortical relay to primary sensory regions ('thalamic gating'[31,32]) or, alternatively, whether it mainly affects cortical signaling beyond primary regions[33].

We capitalized on a unique opportunity to compare auditory responses in neurosurgical epilepsy patients implanted with depth electrodes as they were anesthetized immediately before removal of intracranial electrodes. Recording intracranial field potentials and neuronal spiking activity, we compared auditory responses in wakefulness and light "just-hypnotic" anesthesia, to focus on changes related to LOC. Working with human subjects capable of responding purposefully to verbal tasks allowed us to reliably assess the moment of LOC. High-fidelity auditory responses evident in individual trials enabled comparison of sensory responses in short intervals immediately before and after LOC, thereby isolating the changes most relevant to LOC and minimizing confounding effects of deep anesthesia (e.g. changes in breathing, blood circulation, and thermoregulation). Our results reveal that anesthesia-induced LOC disrupts auditory responses in association cortex, while significant early responses in primary auditory cortex are relatively preserved. This distinction was observed for both simple (click-train) and complex (word) stimuli, and evident in LFPs as well as in

single-neuron spiking activity representing neuronal output.

Results

To study the effects of anesthesia-induced LOC on sensory-evoked neuronal activity in humans, we recorded intracranial EEG (iEEG), Local Field Potentials (LFPs), and neuronal spiking activity in epilepsy patients implanted with depth electrodes (Fig. 1a,b) or subdural cortical grids/strips, as they were anesthetized immediately before removal of intracranial electrodes. In nine experimental sessions (Supplementary Table 1), individuals listened to 40Hz click trains, and from the third session onwards, they were also presented with words and performed an auditory detection task. During each session the subjects were gradually anesthetized with propofol (Fig. 1c,d & Supplementary Figs. 1,2). To concentrate on changes in brain activity specifically related to LOC rather than to deep anesthesia, we used bispectral index (BIS) monitoring to exclude recordings deeper than the midpoint of the anesthetic range (BIS < 50, Fig. 1e)[34]. We operationalized LOC as loss of behavioral responsiveness (LOR) on our task. Of note, the American Society of Anesthesiology (ASA) clinically defines such light anesthesia (characterized by unresponsiveness to verbal commands) as "deep sedation". In each session, we compared auditory responses recorded in the first few minutes after LOR ('anesthesia', average BIS = 67, n = 9) with those recorded in an equally long interval during propofol-free wakefulness ('wakefulness', Fig. 1e, average BIS = 95).

Anesthesia-induced LOC disrupts responses in association cortex

In wakefulness, 40Hz click-trains (Fig. 2a top & Methods) strongly entrained field potentials such that time-locked iEEG responses were highly coherent across single trials (Fig. 2a). We quantified the response fidelity of each iEEG electrode (n = 612) by calculating its Inter Trial Phase Coherence (ITPC, Methods, and Supplementary Figure 3) at 40Hz. During wakefulness (Fig. 2b), significant responses (p<0.01) were found in 66% of contacts (median ITPC of all

6

contacts = 0.40, median p = 4×10^{-5}, n = 612). Responses were observed across all cortical lobes yet exhibited spatial selectivity, with temporal contacts around auditory cortex showing the strongest responses. During anesthesia, iEEG responses in association cortices were markedly reduced (Fig. 2c,d). Accordingly, 65% of responding electrodes (n = 421) showed significant reduction in ITPC (p<0.05, Monte Carlo permutation test) compared to only 1.0% showing significant increase in ITPC. Robust attenuation was also evident when quantifying the distribution of gain factors between states (Methods), which was strongly skewed towards attenuation upon LOC (Fig. 2e). During anesthesia, significant (p<0.01) responses persisted in only 22% of contacts (median ITPC of all contacts = 0.17, median p = 0.20, n = 612) and 95% of these responses were observed in electrodes close to auditory cortex. Even in iEEG contacts located closest to PAC (on the shafts targeted towards the PAC), response fidelity was markedly reduced upon anesthetic-LOC (median ITPC dropped from 0.83 to 0.37, n = 27; 85% of such responsive electrodes significantly reduced ITPC compared to none showing significant increase). Disruption of iEEG responses in association cortices upon LOC was highly reproducible across individual sessions (Supplementary Fig. 4), and evident also when quantifying responses through event-related spectral power (ERSP, "induced power", Supplementary Fig. 5).

Robust responses persist after LOC in primary auditory cortex

In five sessions, microwires targeted seven regions located more medially in and around Heschl's gyrus and recorded locally referenced LFPs (n = 56 microwires). Four of the seven regions (Fig. 3, regions A-D) were located in Heschl's gyrus and exhibited short-latency (<30ms) responses (Supplementary Fig. 6). For brevity, we refer to these as "Primary Auditory Cortex (PAC)" throughout, despite the lack of systematic tonotopic mapping for delineating

7

A1 (Methods). In contrast to disrupted iEEG responses in association cortices, PAC LFPs continued to show highly significant responses during anesthetic-LOC (Fig. 3a,b; median ITPC = 0.73, n = 32, $p<10^{-15}$). Accordingly, the distribution of gain factors between states was largely symmetrical and only showed modest attenuation (Fig. 3c), a pattern significantly different from that found in association cortices ($p<10^{-12}$, n_{AC} = 421, n_{PAC} = 32). Importantly, the distinction between persistent responses in PAC (median gain = -0.15, n = 32) and significant attenuation in adjacent iEEG electrodes (median gain = -0.47, n = 8) was evident when comparing these profiles in simultaneously recorded data (p = $6x10^{-3}$ by Wilcoxon rank-sum test, n_{PAC} = 32, n_{iEEG} = 8).

Preserved PAC responses were also observed in the neuronal spiking responses to words (n = 77 responses in 34 units). Fig. 3d shows a representative PAC neuron (see Supplementary Fig. 7 for additional examples), where firing rate responses were essentially unchanged between wakefulness and anesthetic-LOC. A quantitative analysis across all responses (Fig. 3e, Methods) confirmed that most (68%) PAC responses did not significantly change between wakefulness and anesthetic-LOC (p>0.05, Wilcoxon rank-sum test). Similarly, components showing attenuation (14%) or potentiation (18%) were roughly equally prevalent, indicating a preservation of PAC spike responses, as was the case for PAC LFPs.

Higher-order auditory regions exhibit variable effects upon anesthetic-LOC with spike responses largely attenuated

We refer to temporal lobe regions outside PAC with higher latencies and/or weaker responses during wakefulness as higher-order auditory regions (Regions E-G, Supplementary Fig. 6, and Methods).

8

Region E (response latency 52ms vs. 17ms in PAC, Supplementary Fig. 6), exhibited highly reproducible auditory responses in wakefulness (Fig. 4a & 4b; median ITPC = 0.84, median p < 10^{-21}, n = 8), which dramatically attenuated to noise levels after anesthetic-LOC (Fig. 4b & 4c/top; median ITPC = 0.15, median p = 0.20), as observed in association cortices (Fig. 4c/top). In line with LFP attenuation, neuronal spiking responses to words in this region (n = 56 responses in 9 units) strongly dropped around LOC. Fig. 4d shows a representative neuronal response, demonstrating clear attenuation in firing response to a word stimulus upon anesthetic-LOC (see Supplementary Fig. 7 for additional examples). A quantitative analysis across all responses (Fig. 4e) showed strong response suppression, with 84% of responses significantly attenuating (p<0.05), 16% showing no significant change, and none showing potentiation.

Regions F & G showed a different response profile consisting of weak, albeit significant auditory responses in wakefulness (Fig. 4b; median ITPC = 0.25, n = 16, p = 3×10^{-3}), which moderately strengthened upon anesthetic-LOC (Fig. 4b & 4c/top, median ITPC = 0.36, median p < 10^{-5}). Here, 42% of microwires showed significant potentiation (p<0.05), and none showed attenuation. Anecdotally, the responses of one auditory-responsive neuron identified in these regions (Supplementary Fig. 8 bottom right) were moderately potentiated, agreeing with the LFP results. Altogether, the effects of anesthetic-LOC in higher-order auditory regions were variable, but the strongest high-fidelity responses and corresponding spiking activities were significantly attenuated.

Induced power responses to words during wakefulness and upon anesthetic-LOC

Induced gamma-band (40-200Hz) power is an established and widely-used proxy for neuronal activity in local neuronal populations[35]. We therefore sought to measure how anesthetic-LOC

affected gamma power induced by words in both iEEG and LFP signals. We identified 50 iEEG contacts and 34 microwires that showed a significant gamma response in either wakefulness or anesthesia ($p<0.005$, Wilcoxon signed-rank, Methods), all of which were located in the temporal lobe (Fig. 5). Figure 5a shows a representative induced power response in an iEEG electrode. Upon anesthetic-LOC, the gamma response increased its power, decreased its peak spectral frequency, and the concomitant decrease in power below 20Hz (often referred to as alpha/beta desynchronization[36]) was largely absent. A quantitative analysis across the entire dataset (Methods) confirmed that increased gamma power was a robust phenomenon across auditory-responsive electrodes (Fig. 5b,c,e; 83% increase, $p < 10^{-8}$, n = 50 for iEEGs; 32% increase, $p = 2\times10^{-4}$, n = 34 for LFPs). Similarly, a decrease in peak gamma spectral frequency was evident across electrodes (Fig. 5b,d; 50Hz shift, $p < 10^{-7}$ for iEEGs; 48Hz shift, $p = 3\times10^{-5}$ for LFPs). Since gamma power increase was consistently observed upon anesthetic-LOC, independently of changes in neuronal firing rates (that often showed attenuation), we examined to what extent gamma modulations caused by anesthetic-LOC were correlated with modulations in simultaneously recorded spiking responses on the same microwires. There was little or no correlation between anesthetic-LOC modulated gamma power and spiking responses (r = -0.06, n = 81). By contrast, time-locked LFP responses to 40Hz click trains as captured by ITPC were correlated with spiking responses on the same microwires (r = 0.61, n = 124). Finally, upon LOC the 10-20Hz power decrease (alpha/beta desynchronization) was consistently reduced in iEEG data (Fig. 5b, left, $p = 8\times10^{-4}$, n = 50), but a significant reduction was not observed in LFPs (Fig. 5b, right, p = 0.08, n = 34). Taken together, anesthetic-LOC causes complex changes in induced power including gamma power increase and slowing of spectral frequency profiles, which can be decoupled from local spiking activities after LOC (see also Discussion).

10

Discussion

By studying human auditory responses during the descent to anesthesia, we show that anesthesia-induced LOC is associated with robust disruption of auditory responses in association cortex, while significant early PAC responses persist. LOC was consistently associated with response breakdown across wide cortical territories (Fig. 2 & Supplementary Fig. 4,5). By contrast, both LFP and spike responses in PAC (Fig. 3) consistently showed robust responses after LOC. The distinction between PAC and association cortices was evident in response to both simple 40Hz click-trains and complex word stimuli. In intermediate high-order auditory regions effects were variable, and spiking responses largely attenuated around LOC (Fig. 4). Interestingly, gamma power induced by words increased after LOC while its frequency profile slowed, but such power increase did not correlate with changes in neuronal firing on the same microwires.

Since the study was conducted in neurosurgical epilepsy patients, it inherently entails some limitations that should be explicitly acknowledged. We cannot completely rule out the contribution of epileptogenic activity. In addition, the number of participants implanted with electrodes in auditory regions that volunteer to participate in research during brain surgery is limited, as is the number of recorded neurons. However, the highly consistent results across patients with different clinical profiles largely overcome these limitations. Another possible concern is that the precise brain regions targeted and the anesthesia protocols vary between sessions, as they are guided by clinical criteria. We addressed this by employing a within-session design and defining the anesthesia interval according to the same clinical endpoint (LOR) across all sessions. Furthermore, the same anesthetic agent (propofol) was used for all

11

sessions. Future studies will determine the extent to which these findings generalize to other anesthetic agents.

In contrast to the "thalamic gating" hypothesis whereby the relay to primary sensory regions is disrupted[32], our results support the notion of preserved PAC responses under light anesthesia[23,27,37], as was also found for LFP responses to visual stimulation[15]. A recent study examining the effects of propofol on human LFP auditory responses reported preserved early evoked potentials in the most posteromedial part of Heschl's gyrus when compared to intermediate and anterolateral regions showing robust attenuation[38]. Our study extends this observation along several dimensions, such as examining responses across wide territories including fronto-parietal cortices. Most importantly, we recorded spike responses to complex word stimuli. The contribution of these data is two-fold: First, it consistently showed similar effects as LFP ITPC results, thereby allowing to extrapolate and confidently interpret time-locked LFP responses as reflecting local spiking activities even when these were not available. Second, it exposed interesting differences after LOC compared with simultaneously recorded gamma power changes. The fact that spiking responses are preserved in PAC is of particular importance since this demonstrates unequivocally that during anesthetic-LOC not only is the synaptic input into PAC preserved, but also the circuit's output. The apparent discrepancy with studies reporting attenuation of PAC responses under anesthesia[20–22] may reflect effects of deep surgical anesthesia unrelated to LOC, and highlights the importance of using "just-hypnotic" anesthesia when studying LOC. While the present results establish preserved PAC responses to isolated stimuli upon anesthesia-induced LOC, they do not preclude potential effects on select neuronal populations, precise spike timing, or contextual effects that require integration across long temporal intervals.

Attenuated EEG responses to 40Hz click-trains have been repeatedly demonstrated upon anesthesia-induced LOC and have been suggested as a useful marker for assessing the depth of anesthesia[25,39]. Our results indicate that disruption of scalp EEG responses represent attenuated activity in association cortices, as can be expected given that preserved PAC responses only modestly contribute to total cerebral activity, and given the medial location of PAC that is less accessible to non-invasive scalp EEG. Indeed, our own iEEG results show robust attenuation upon anesthesia-induced LOC (Fig. 2). The effectiveness of the specific 40Hz click-train stimulus in revealing correlations with LOC may be related to an inability of large neuronal populations to reliably synchronize coherently with high-frequency stimulation in disconnected states[40]. Studies in natural sleep demonstrate a similar distinction between preserved tracking of acoustic properties and PAC responses[41] vs. high-order activity in association cortex[42]. Thus, a functional disconnection between primary sensory and association cortex may be a general property of LOC not only due to anesthesia, as demonstrated also by direct perturbation of cortical activity with transcranial magnetic stimulation (TMS)[43–45]. In addition, our results join findings from other lines of research showing that when sensory stimuli are not perceived, activity in primary sensory regions is largely preserved whereas activity in association cortices is attenuated[46–49].

Our findings reveal complex effects on induced power changes, where anesthetic-LOC was associated with gamma power increase and a slowing of frequency profiles (Fig. 5). Such changes are in line with previous studies showing that anesthesia/sedation increases gamma responses power in-vitro[50] and in humans in-vivo[51,52]. Similarly, a slowing of spectral frequencies upon anesthesia has been observed in-vitro[50,53], and in monkeys[54] and humans

13

in-vivo[52]. Our results show that the relation between induced gamma power and local spiking activity may change across states, but the extent of potential decoupling between gamma activity and neuronal firing remains unclear, and we can only speculate about its underlying source. One possibility is that these two measures emphasize the contribution of different neuronal populations that diverge upon anesthetic-LOC. For example, gamma oscillations are closely coupled with inhibitory GABAergic interneurons[55], whilst extracellular recordings mostly capture excitatory pyramidal cells[56]. Differences may also stem from differential contributions from distinct cortical layers or cell populations at different spatial scales. We also find that stimulus-induced decrease in 10-20Hz power (prevalent during wakefulness) diminishes upon anesthetic-LOC (Fig. 5). Given that alpha/beta desynchronization has been linked with top-down signaling [57], this may support the notion that anesthesia predominantly affects top-down signaling [23,58].

What could be the mechanisms by which LOC disrupts effective cortical functional connectivity? Anesthesia is likely to exert its effects by affecting endogenous subcortical sleep/wake centers that modulate thalamocortical activity[2,59]. Accordingly, the distribution of modulatory receptors may differ between primary sensory regions and association cortices, rendering the latter unresponsive to preserved ascending input. An alternative explanation for the inability to effectively drive responses in association cortices may reflect a disruption to indirect cortico-thalamo-cortical pathways linking cortical regions via high-order thalamic nuclei[60,61]. Thus, refining the traditional "thalamic gating" notion from disruption of primary relay nuclei, to focus on high-order thalamic nuclei, could reconcile the present results with the well-established effect of anesthesia reducing thalamic activity[32]. Alternatively, our findings may reflect a "multiple hit mechanism", whereby anesthesia causes multiple small

14

perturbations at each step in the sensory processing chain. The sum of these perturbations may seem modest in the PAC as measured with current methods, but may have accumulated sufficiently to be noticeable in the higher association cortices. Finally, anesthetics could affect top-down signaling that may be more dominant in association cortices[58,62], possibly involving specific ion channels that link bottom-up and top-down signaling[63]. Beyond the specific mechanisms at play, the disruption of effective cortical connectivity is consistent with a number of theoretical perspectives[64,65].

In conclusion, our findings demonstrate that anesthesia-induced LOC disrupts auditory responses beyond primary cortex while significant responses persist in PAC. The fact that the major disruption in sensory signaling upon LOC occurs after primary cortices highlights impaired effective cortical connectivity as a key factor in LOC, a factor that should guide future mechanistic research of LOC as well as anesthesia improvements and monitoring schemes.

15

Online Methods

Subjects

Eight patients (six male, see Supplementary Table 1 for details) with intractable drug-resistant epilepsy were implanted with chronic depth electrodes, or subdural cortical grids and strips (one session), for 7-10 days, to identify seizure foci for potential surgical treatment. Electrode location and anesthesia management (below) were based solely on clinical criteria. One patient was implanted on two different occasions due to inconclusive clinical results from the first hospital admission. All patients provided written informed consent to participate in the research study, under the approval of the Institutional Review Board at Tel Aviv Sourasky Medical Center, or the University of Bonn Epileptology Department (one individual). Data were collected prior to removal of the electrodes under anesthesia at the end of monitoring on the medical ward.

Anesthesia

Standard anesthesia monitoring was performed according to the guidelines set by the American Society of Anesthesiologists (ASA), complemented with bispectral index monitoring[34] (BIS VISTA™ Monitoring System, Medtronic, Boulder, CO, USA). Propofol was infused using a simple (non-Target Controlled Infusion) syringe pump, with infusion rates increasing in a step-wise fashion over 20-40 minutes (5 to 400 µg/kg/min) to achieve anesthesia whilst maintaining spontaneous ventilation. In two sessions (see Supplementary Table 1) adjuvant agents (fentanyl, midazolam or remifentanil) were given according to the discretion of the anesthesiologist. When a sufficient depth of anesthesia was achieved (as determined by the anesthesiologist, aiming to avoid movement in response to painful stimulus whilst maintaining spontaneous ventilation), recordings were stopped and the

16

neurosurgeons removed the electrodes. Post-hoc pharmacokinetic and pharmacodynamic modelling using the three-compartment Marsh Model[66–69] (Supplementary Fig. 1), were used to estimate the momentary effect-site concentration of propofol in brain tissue (Fig. 1 and Supplementary Fig. 2).

Auditory Paradigm

Auditory stimuli were continuously presented throughout the descent to anesthesia (20 – 70 minutes) using headphones (8 sessions) or speakers (1 session), with sound intensity levels adjusted at the start of each session to be comfortably audible. 40Hz click-trains (duration = 500ms, 21 clicks) were presented in all recording sessions. Additionally, up to seven word stimuli (duration = 500ms - 600ms), including one task target (duration 500ms), were presented in seven sessions. Auditory stimuli were presented in a pseudorandom order, at 1.5s intervals (± 400ms jitter). Patients were instructed to press a response button upon hearing a specific target word, to determine the moment of loss of responsiveness under anesthesia.

Electrophysiology

In eight sessions, patients had been implanted with 5 – 11 depth electrodes targeting different brain regions (Fig. 1B), whereby each electrode consisted of eight platinum iEEG contacts along their shaft, eight additional microwires protruding a few mm from the distal tip, and a 9th low-impedance reference microwire[70]. In one of these sessions iEEG only data was available, and in a further, ninth session a patient was implanted with a combination of two two-dimensional subdural electrocorticography (ECoG) grid arrays and four one-dimensional subdural ECoG strips. Data were recorded using either Blackrock (Salt Lake City,

17

UT, USA) or Neuralynx (Bozeman, MT, USA) data acquisition systems. Microwire data were

sampled at 30kHz (Blackrock) or 32,768 Hz (Neuralynx) and referenced to the local low

impedance 9th microwire on each electrode, or in one session to a single low impedance 9th

microwire (session 6, see Supplementary Table 1). iEEG and ECoG data were sampled at 2 kHz

(Blackrock) or 2,048 Hz (Neuralynx) and referenced to a central scalp electrode (Cz).

Electrode Localization

Pre-implant MRI scans (Siemens Prisma scanner or GE Signa scanner, 3 Tesla, T1 sequence,

resolution 1mm x 1mm x 1mm) were co-registered with post-implant CT scans (Philips

MX8000 or Brilliance, resolution 1.5mm x 0.5mm x 0.5mm or 0.75mm x 0.5 mm x 0.5mm) to

identify locations of electrodes. Individual subject data were further transformed into

Talairach space[71] to facilitate simultaneous visualization of electrode positions in different

individuals. To this end, electrode locations were marked with 5mm spheres on the standard

brain, and intersections with the grey-white matter boundary surface were identified. The

cortical surface was then inflated and flattened by unfolding and cutting along the calcarine

sulcus and predefined medial anatomical landmarks (Supplementary Fig. 4). When plotted on

folded grey-white matter boundary surface (Fig. 2, Fig. 5 & Supplementary Fig. 5), the location

of each electrode was defined as the center of mass of the intersection of the 5mm sphere

with the surface, and a circle was drawn in that location (minimal jitter was introduced to

allow visualization and avoid hidden data).

Defining "Wakefulness" vs. "Anesthesia" Periods

To compare auditory responses during propofol-free wakefulness to those under light

anesthesia (formally defined by the ASA as "deep sedation": unresponsiveness to simple

verbal instructions) we defined the anesthesia period as the first eight minutes following LOR for which BIS>50 (to avoid deep anesthesia). Supplementary Table 1 and Supplementary Fig. 2 provide full details regarding recording durations and definitions of wakefulness and anesthesia intervals in each session. LOR was defined as the midpoint between the last correct behavioral response and the following missed target word. For each experimental session, we chose an interval of propofol-free wakefulness with identical duration for a within-session comparison. In two sessions the anesthesia period was truncated to avoid deep anesthesia (sessions 7 & 8). Whenever eight minutes were not available for either wakefulness or anesthesia, we used the longest possible noise-free intervals with identical durations in both wakefulness and anesthesia (Supplementary Fig. 2 & Supplementary Table 1). Average BIS values quoted in the text were calculated by integrating over BIS curves during wakefulness or anesthesia for each session (with linear interpolation between known data points), and then taking the median across sessions.

Analysis of iEEG/LFP responses to 40Hz click trains

Responses to 40Hz click trains were quantified using Inter-Trial Phase Coherence (ITPC, Fig. 2 & 3), also known as the "phase-locking factor"[72,73]:

$$ITPC = \left| \frac{1}{N} \sum_{k=1}^{N} e^{i\phi_k} \right|$$

where N signifies the number of trials, and ϕ_k the phase of the spectral estimate for trial k for the 40Hz frequency

The statistical significance values associated with ITPC were estimated as in Zar (1999)[74] with a significance threshold of $\alpha = 0.01$. Quoted averages of ITPC p-values are the median of these

p-value estimates. Median ITPC values for Supplementary Fig. 4 were calculated on the 421 iEEG electrodes showing significant ITPC in either wakefulness or anesthesia.

The gain factor between wakefulness and anesthesia was calculated as in as in[41,75]:

$$Gain = \frac{R_{Anesthetized} - R_{Awake}}{max\left(R_{Anesthetized}, R_{Awake}\right)}$$

where $R_{Anesthetized}$ and R_{Awake} is the ITPC for a particular channel during wakefulness or anesthesia.

Additionally, responses were quantified by calculating the Event-Related Spectral Power (ERSP) at 40Hz (Supplementary Fig. 5), reflecting power modulations that are not necessarily phase-locked and known also as "induced power". To this end, the 40Hz spectral power was calculated by applying a Hann window over the 500ms of the response (or baseline) iEEG/LFP signal, and calculating the squared 40Hz amplitude component of the Fourier transform. Spectral power during baseline was subtracted from that during response, and the result divided by the median baseline spectral power at 40Hz. This ERSP was averaged across all trials for each electrode (Supplementary Fig. 5). Statistical significance of ERSP responses was calculated using a Wilcoxon signed-rank test, with significance level of α = 0.01 (non-significant values are masked in brown in Supplementary Fig. 5).

Response latency. Latency (Supplementary Fig. 6b) was calculated based on the locally referenced LFP response to the 40 Hz click train during wakefulness for each individual microwire targeted around Heschl's Gyrus (Fig. 3 & 4). This method requires responses to be

20

strongly coherent between trials, and was possible to implement in 72% of auditory-responsive electrodes with ITPC > 0.5 (most of which were > 0.85). The mean LFP response ([-600,2000]ms from stimulus onset) to 40 Hz click train was bandpassed at 30-150Hz (4th order zero-phase-shift digital butterworth filter) to include the LFP response at 40 Hz and its harmonics. Then, its envelope was extracted using the Hilbert transform. Using a 525 ms length moving window (window size was chosen to match the LFP response to the stimulus of 21 clicks with 25 ms ISI), latency was defined as the onset time of the window where the largest mean envelope was obtained.

LFP induced power response to words. Responses were quantified by measuring, for each microwire and iEEG contact, the event-related gamma power (40-200Hz, mean of FFT magnitudes squared) for each trial across words (100-500ms Hann window, post-trial onset) and comparing it with power during the corresponding pre-stimulus baseline period (-450 to -50 ms). "Responding channels" were defined as those in which this gamma power during response was significantly different from baseline gamma power ($p<0.005$, Wilcoxon signed-rank), and were selected for further analysis. Response power spectra for each responding channel were calculated by dividing the event-related power in each trial (100-500ms) at each frequency, by the corresponding baseline power, and then taking the median across wakefulness (or anesthesia) trials. This spectrum per channel was then averaged (mean ±SEM) across iEEG or microwire channels to visualize the grand mean profile (Fig. 5b). The peak spectral power during wakefulness or anesthesia was determined for each channel separately by identifying the highest peak in the power spectrum, and finding its power (Fig. 5c) and frequency (Fig. 5e). The alpha/beta desynchronization trough power during wakefulness or anesthesia was determined for each channel by identifying the deepest

21

trough in the power spectrum that was to the left of (lower frequency than) the peak power above, and which also lay below 50Hz. On occasions where no such trough was identified, the alpha/beta desynchronization was assumed to have disappeared, and the trough value was set to zero dB. Gain factors between wakefulness and anesthetic-LOC for gamma power (Fig. 5d) were calculated in each channel separately as follows. Event-related gamma power change compared to baseline (as described above) was normalized by dividing by the median baseline power across trials, and averaged over awake (or anesthesia) trials, yielding a "gamma power response" for that channel during wakefulness (or anesthesia). The gain factor was then calculated as described above for ITPC, but substituting $R_{Anesthetized}$ and R_{Awake} with the gamma power response for a particular channel during wakefulness or anesthesia.

Analysis of neuronal spiking activity

Spike sorting was performed using the wave_clus toolbox for Matlab as described previously[76,77]: (i) extracellular microwire recordings were high-pass filtered above 300Hz, (ii) a 5 × SD-approximation ($median\{|data|/0.6745\}$) threshold above the median noise level was computed, (iii) detected events were clustered using superparamagnetic clustering, and categorized as noise, single- or multi-unit clusters. Classification of single- and multi-unit clusters was based on the consistency of action potential waveforms, and by the presence of a refractory period for single units, i.e. less than 1% of inter-spike-intervals (ISIs) within 3ms. Raster and peri-stimulus time histograms (PSTH) were produced for each neuronal unit in response to each word (see Supplementary Fig. 7 for examples). Instantaneous firing rate traces (all PSTHs below raster plots) were calculated by smoothing the binary spike trains with a Gaussian kernel (σ = 5 ms). Raster plots were inspected manually, and periods of increased firing above baseline were identified as "response components" (black arrows in

Supplementary Fig. 7). A single unit responding to a few isolated acoustic events (e.g. phonemes) within a single word stimulus could therefore have one or more response components (Supplementary Fig. 7), and the firing rate (total spikes) of each such component was compared separately between wakefulness and anesthesia. Categorization of response components as potentiated, attenuated or unchanged was determined via a Wilcoxon rank-sum test with a significance level of α = 0.05.

Statistics. P-values were calculated using Wilcoxon rank-sum tests, Wilcoxon signed-rank tests, or Monte Carlo permutation tests, as reported above, while treating iEEG or LFP for different electrodes as independent measures. Error bars in all figures denote standard error of the mean (SEM = SD/$\sqrt{n}$, where n is the number of data points) unless otherwise stated.

Data and code availability

The data that support the findings of this study and the computer code used to generate the results are available from the corresponding author upon reasonable request.

Acknowledgements

Author contributions

I.F. and Y.N. conceived of research.

A.M. and A.J.K designed experiments and analyzed data.

A.J.K, A.M., H.G.S, A.T., F.M. and Y.N. collected data.

I.F., I.S., and J.B. performed surgeries.

D.H., M.S., and I.M. supervised anesthesia.

F.F. supervised clinical care and analyzed epilepsy profiles.

24

A.J.K, A.M., H.G.S, I.F. and Y.N. wrote the manuscript.

All authors provided ongoing critical review of results and commented on the manuscript.

Competing Financial Interests Statement

None to declare.

References

1. Bigelow, H. J. Insensibility during Surgical Operations Produced by Inhalation. *Bost. Med. Surg. J.* **35,** 309–317 (1846).

2. Brown, E., Purdon, P. & Dort, C. Van. General anesthesia and altered states of arousal: A systems neurosciences analysis. *Annu. Rev. Neurosci.* **34,** 601–628 (2011).

3. Brown, E. N., Lydic, R. & Schiff, N. D. General anesthesia, sleep, and coma. *N. Engl. J. Med.* **363,** 2638–2650 (2010).

4. Evers, A. & Crowder, M. in *Clinical anesthesia* (eds. Barash, P. G., Cullen, B. F., Stoelting, R. K., Cahalan, M. & Stock, M. C.) 95–114 (Lippincott Williams & Wilkins, 2006).

5. Campagna, J. A., Miller, K. W. & Forman, S. A. Mechanisms of actions of inhaled anesthetics. *N. Engl. J. Med.* **349,** 909-910; author reply 909-910 (2003).

6. Hemmings, H. C. *et al.* Emerging molecular mechanisms of general anesthetic action. *Trends Pharmacol. Sci.* **26,** 503–510 (2005).

7. Rudolph, U. & Antkowiak, B. Molecular and neuronal substrates for general anaesthetics. *Nat. Rev. Neurosci.* **5,** 709–720 (2004).

8. Kennedy, D. & Norman, C. What don't we know? *Science* **309,** 75 (2005).

9. Franks, N. P. General anaesthesia: from molecular targets to neuronal pathways of sleep and arousal. *Nat. Rev. Neurosci.* **9,** 370–386 (2008).

10. Alkire, M. T., Hudetz, A. G. & Tononi, G. Consciousness and anesthesia. *Science (80-.).* **322,** 876–880 (2008).

11. Mountcastle, V. Modality and Topographic Properties of Single Neurons of Cat's Somatic Sensory Cortex. *J. Neurophysiol.* **20,** 408–434 (1956).

12. Hubel, D. H. & Wiesel, T. N. Receptive fields of single neurones in the cat's striate cortex. *J. Physiol.* **148,** 574–591 (1959).

13. Merzenich, M. M., Knight, P. L. & Roth, G. L. Representation of cochlea within primary auditory cortex in the cat. *J. Neurophysiol.* **38,** 231–249 (1975).

14. Wörgötter, F. *et al.* State-dependent receptive-field restructuring in the visual cortex. *Nature* **396,** 165–168 (1998).

15. Imas, O. a, Ropella, K. M., Ward, B. D., Wood, J. D. & Hudetz, A. G. Volatile anesthetics disrupt frontal-posterior recurrent information transfer at gamma frequencies in rat.

Neurosci. Lett. **387,** 145–50 (2005).

16. Haider, B., Häusser, M. & Carandini, M. Inhibition dominates sensory responses in the awake cortex. *Nature* **493,** 97–102 (2013).

17. Ferezou, I., Bolea, S. & Petersen, C. C. H. Visualizing the Cortical Representation of Whisker Touch: Voltage-Sensitive Dye Imaging in Freely Moving Mice. *Neuron* **50,** 617–629 (2006).

18. Constantinople, C. M. & Bruno, R. M. Effects and mechanisms of wakefulness on local cortical networks. *Neuron* **69,** 1061–1068 (2011).

19. Kleinfeld, D., Ahissar, E. & Diamond, M. E. Active sensation: insights from the rodent vibrissa sensorimotor system. *Curr. Opin. Neurobiol.* **16,** 435–444 (2006).

20. Brugge, J. F. & Merzenich, M. M. Responses of neurons in auditory cortex of the macaque monkey to monaural and binaural stimulation. *J. Neurophysiol.* **36,** 1138–1158 (1973).

21. Evans, E. F. & Whitfield, I. C. Classifcation of unit responses in the auditory cortex of the unanaesthetized and unrestrained cat. *J. Physiol.* **171,** 476–93 (1964).

22. Katsuki, Y., Murata, K., Suga, N. & Takenaka, T. Electrical Activity of Cortical Auditory Neurons of Unanaesthetized and Unrestrained Cat. *Proc. imp. Japan Acad.* **35,** 571–574 (1959).

23. Raz, A. *et al.* Preferential effect of isoflurane on top-down vs. bottom-up pathways in sensory cortex. *Front. Syst. Neurosci.* **8,** 1–22 (2014).

24. Schwender, D., Klasing, S., Madler, C., Pöppel, E. & Peter, K. Depth of anesthesia. Midlatency auditory evoked potentials and cognitive function during general anesthesia. *Int. Anesth. Clin.* **31,** 89–106 (1993).

25. Plourde, G. The effects of propofol on the 40-Hz auditory steady-state response and on the electroencephalogram in humans. *Anesth. Analg.* **82,** 1015–1022 (1996).

26. Dueck, M. H. *et al.* Propofol attenuates responses of the auditory cortex to acoustic stimulation in a dose-dependent manner: A FMRI study. *Acta Anaesthesiol. Scand.* **49,** 784–791 (2005).

27. Davis, M. H. *et al.* Dissociating speech perception and comprehension at reduced levels of awareness. *Proc. Natl. Acad. Sci. U. S. A.* **104,** 16032–16037 (2007).

28. Heinke, W. *et al.* Sequential effects of propofol on functional brain activation induced by auditory language processing: An event-related functional magnetic resonance

imaging study. *Br. J. Anaesth.* **92,** 641–650 (2004).

29.   Austin, V. C. *et al.* Confounding effects of anesthesia on functional activation in
rodent brain: A study of halothane and α-chloralose anesthesia. *Neuroimage* **24,** 92–
100 (2005).

30.   Heinke, W. & Schwarzbauer, C. In vivo imaging of anaesthetic action in humans:
Approaches with positron emission tomography (PET) and functional magnetic
resonance imaging (fMRI). *Br. J. Anaesth.* **89,** 112–122 (2002).

31.   Llinas, R. R. & Steriade, M. Bursting of Thalamic Neurons and States of Vigilance. *J.
Neurophysiol.* **95,** 3297–3308 (2006).

32.   Alkire, M. T., Haier, R. J. & Fallon, J. H. Toward a unified theory of narcosis: brain
imaging evidence for a thalamocortical switch as the neurophysiologic basis of
anesthetic-induced unconsciousness. *Conscious. Cogn.* **9,** 370–386 (2000).

33.   Flores, F. J. *et al.* Thalamocortical synchronization during induction and emergence
from propofol-induced unconsciousness. *Proc. Natl. Acad. Sci.* 201700148 (2017).
doi:10.1073/pnas.1700148114

34.   Kelley, S. D. *Monitoring Counsciousness Using the Bispectral Index Using the
Bispectral index* ^{TM} *During Anesthesia*. (Covidien, 6135 Gunbarrel Ave, Boulder, CO,
USA, 2010).

35.   Nir, Y. *et al.* Coupling between neuronal firing rate, gamma LFP, and BOLD fMRI is
related to interneuronal correlations. *Curr. Biol.* **17,** 1275–1285 (2007).

36.   Pfurtscheller, G. & Aranibar, A. Event-related cortical desynchronization detected by
power measurements of scalp EEG. *Electroencephalogr. Clin. Neurophysiol.* **42,** 817–
826 (1977).

37.   Liu, X. *et al.* Propofol disrupts functional interactions between sensory and high-order
processing of auditory verbal memory. *Hum. Brain Mapp.* **33,** 2487–2498 (2012).

38.   Nourski, K. V. *et al.* Electrocorticographic delineation of human auditory cortical fields
based on effects of propofol anesthesia. *Neuroimage* **152,** 78–93 (2017).

39.   Yli-hankala, A., Edmonds, H. L., Heine, M. F., Strickland, T. & Tsueda, K. Auditory
steady-state response, upper facial EMG, EEG and heart rate as predictors of
movement during isoflurane-nitrous oxide anaesthesia. *Br. J. Anaesth.* **73,** 174–179
(1994).

40.   Sharon, O. & Nir, Y. Attenuated Fast Steady-State Visual Evoked Potentials During

Human Sleep. *Cereb. Cortex* 1–15 (2017). doi:10.1093/cercor/bhx322

41.   Nir, Y., Vyazovskiy, V. V., Cirelli, C., Banks, M. I. & Tononi, G. Auditory responses and stimulus-specific adaptation in rat auditory cortex are preserved across NREM and REM sleep. *Cereb. Cortex* **25,** 1362–1378 (2015).

42.   Makov, S. *et al.* Sleep Disrupts High-Level Speech Parsing Despite Significant Basic Auditory Processing. *J. Neurosci.* **37,** 7772–7781 (2017).

43.   Massimini, M. *et al.* Breakdown of cortical effective connectivity during sleep. *Science (80-.).* **309,** 2228–2232 (2005).

44.   Ferrarelli, F. *et al.* Breakdown in cortical effective connectivity during midazolam-induced loss of consciousness. *Proc. Natl. Acad. Sci. U. S. A.* **107,** 2681–2686 (2010).

45.   Sarasso, S. *et al.* Consciousness and complexity during unresponsiveness induced by propofol, xenon, and ketamine. *Curr. Biol.* **25,** 3099–3105 (2015).

46.   Blake, R. & Logothetis, N. K. Visual competition. *Nat. Rev. Neurosci.* **3,** 13–21 (2002).

47.   Leopold, D. a. & Logothetis, N. K. Activity changes in early visual cortex reflect monkeys' percepts during binocular rivalry. *Nature* **379,** 549–553 (1996).

48.   Sachidhanandam, S., Sreenivasan, V., Kyriakatos, A., Kremer, Y. & Petersen, C. C. H. Membrane potential correlates of sensory perception in mouse barrel cortex. *Nat. Neurosci.* **16,** 1671–1677 (2013).

49.   Gelbard-Sagiv, H., Magidov, E., Sharon, H., Hendler, T. & Nir, Y. Noradrenaline modulates visual perception and late visually-evoked activity.

50.   Oke, O. O. *et al.* High-frequency gamma oscillations coexist with low-frequency gamma oscillations in the rat visual cortex in vitro. *Eur. J. Neurosci.* **31,** 1435–1445 (2010).

51.   Saxena, N. *et al.* Enhanced Stimulus-Induced Gamma Activity in Humans during Propofol-Induced Sedation. *PLoS One* **8,** 1–7 (2013).

52.   Lozano-Soldevilla, D., Ter Huurne, N., Cools, R. & Jensen, O. GABAergic modulation of visual gamma and alpha oscillations and its consequences for working memory performance. *Curr. Biol.* **24,** 2878–2887 (2014).

53.   Whittington, M. a., Jefferys, T. G. R. & Traub, R. D. D. Effects of intravenous anaesthetic agents on fast inhibitory oscillations in the rat hippocampus in vitro. *Br. J. Pharmacol.* **118,** 1977–1986 (1996).

54.   Xing, D. *et al.* Stochastic Generation of Gamma-Band Activity in Primary Visual Cortex

of Awake and Anesthetized Monkeys. *J. Neurosci.* **32,** 13873–13880a (2012).

55. Bartos, M., Vida, I. & Jonas, P. Synaptic mechanisms of synchronized gamma oscillations in inhibitory interneuron networks. *Nat. Rev. Neurosci.* **8,** 45–56 (2007).

56. Viskontas, I. V., Ekstrom, A. D., Wilson, C. L. & Fried, I. Characterizing Interneuron and Pyramidal Cells in the Human Medial Temporal Lobe In Vivo Using Extracellular Recordings. *Hippocampus* **17,** 49–57 (2007).

57. van Kerkoerle, T. *et al.* Alpha and gamma oscillations characterize feedback and feedforward processing in monkey visual cortex. *Proc. Natl. Acad. Sci.* **111,** 14332–41 (2014).

58. Mashour, G. A. Top-down mechanisms of anesthetic-induced unconsciousness. *Front. Syst. Neurosci.* **8,** 1–10 (2014).

59. Devor, M. & Zalkind, V. Reversible analgesia, atonia, and loss of consciousness on bilateral intracerebral microinjection of pentobarbital. *Pain* **94,** 101–112 (2001).

60. Baker, R. *et al.* Altered Activity in the Central Medial Thalamus Precedes Changes in the Neocortex during Transitions into Both Sleep and Propofol Anesthesia. *J. Neurosci.* **34,** 13326–13335 (2014).

61. Theyel, B. B., Llano, D. A. & Sherman, S. M. The corticothalamocortical circuit drives higher-order cortex in the mouse. *Nat. Neurosci.* **13,** 84–88 (2010).

62. Gilbert, C. D. & Sigman, M. Brain States: Top-Down Influences in Sensory Processing. *Neuron* **54,** 677–696 (2007).

63. Phillips, W. A., Larkum, M. E., Harley, C. W. & Silverstein, S. M. The effects of arousal on apical amplification and conscious state. *Neurosci. Conscious.* **2016,** niw015 (2016).

64. Tononi, G., Boly, M., Massimini, M. & Koch, C. Integrated information theory: From consciousness to its physical substrate. *Nat. Rev. Neurosci.* **17,** 450–461 (2016).

65. Dehaene, S. & Changeux, J.-P. Experimental and theoretical approaches to conscious processing. *Neuron* **70,** 200–27 (2011).

66. Marsh, B., White, M., Morton, N. & Kenny, G. N. Pharmacokinetic model driven infusion of propofol in children. *Br. J. Anaesth.* **67,** 41–8 (1991).

67. Absalom, A. R., Mani, V., De Smet, T. & Struys, M. M. R. F. Pharmacokinetic models for propofol- Defining and illuminating the devil in the detail. *Br. J. Anaesth.* **103,** 26–37 (2009).

68.   Cascone, S., Lamberti, G., Titomanlio, G. & Piazza, O. Pharmacokinetics of Remifentanil: a three-compartmental modeling approach. *Transl. Med. @ UniSa* **7,** 18–22 (2013).

69.   ALARIS. *Arsena PK Syringe Pump Manual*. (Alaris Medical Systems, 2004).

70.   Fried, I. *et al.* Cerebral microdialysis combined with single-neuron and electroencephalographic recording in neurosurgical patients. Technical note. *J. Neurosurg.* **91,** 697–705 (1999).

71.   Talairach, J. & Tournoux, P. *Co-Planar Stereotaxic Atlas of the Human Brain: 3-Dimensional Proportional System: An Approach to Cerebral Imaging*. (Thieme Medical Publishers, 1988).

72.   Makeig, S., Debener, S., Onton, J. & Delorme, A. Mining event-related brain dynamics. *Trends Cogn. Sci.* **8,** 204–210 (2004).

73.   Tallon-Baudry, C., Bertrand, O., Delpuech, C. & Pernier, J. Stimulus specificity of phase-locked and non-phase-locked 40 Hz visual responses in human. *J. Neurosci.* **16,** 4240–9 (1996).

74.   Zar, J. H. in *Biostatistical Analysis* 625 (Prentice Hall, 2010).

75.   Issa, E. B. & Wang, X. Sensory responses during sleep in primate primary and secondary auditory cortex. *J. Neurosci.* **28,** 14467–80 (2008).

76.   Quiroga, R. Q., Nadasdy, Z. & Ben-Shaul, Y. Unsupervised spike detection and sorting with wavelets and superparamagnetic clustering. *Neural Comput.* **16,** 1661–1687 (2004).

77.   Nir, Y. *et al.* Selective neuronal lapses precede human cognitive lapses following sleep deprivation. *Nat. Med.* **23,** 1474–1480 (2017).

Figures and legends

Figure 1. Experimental setup
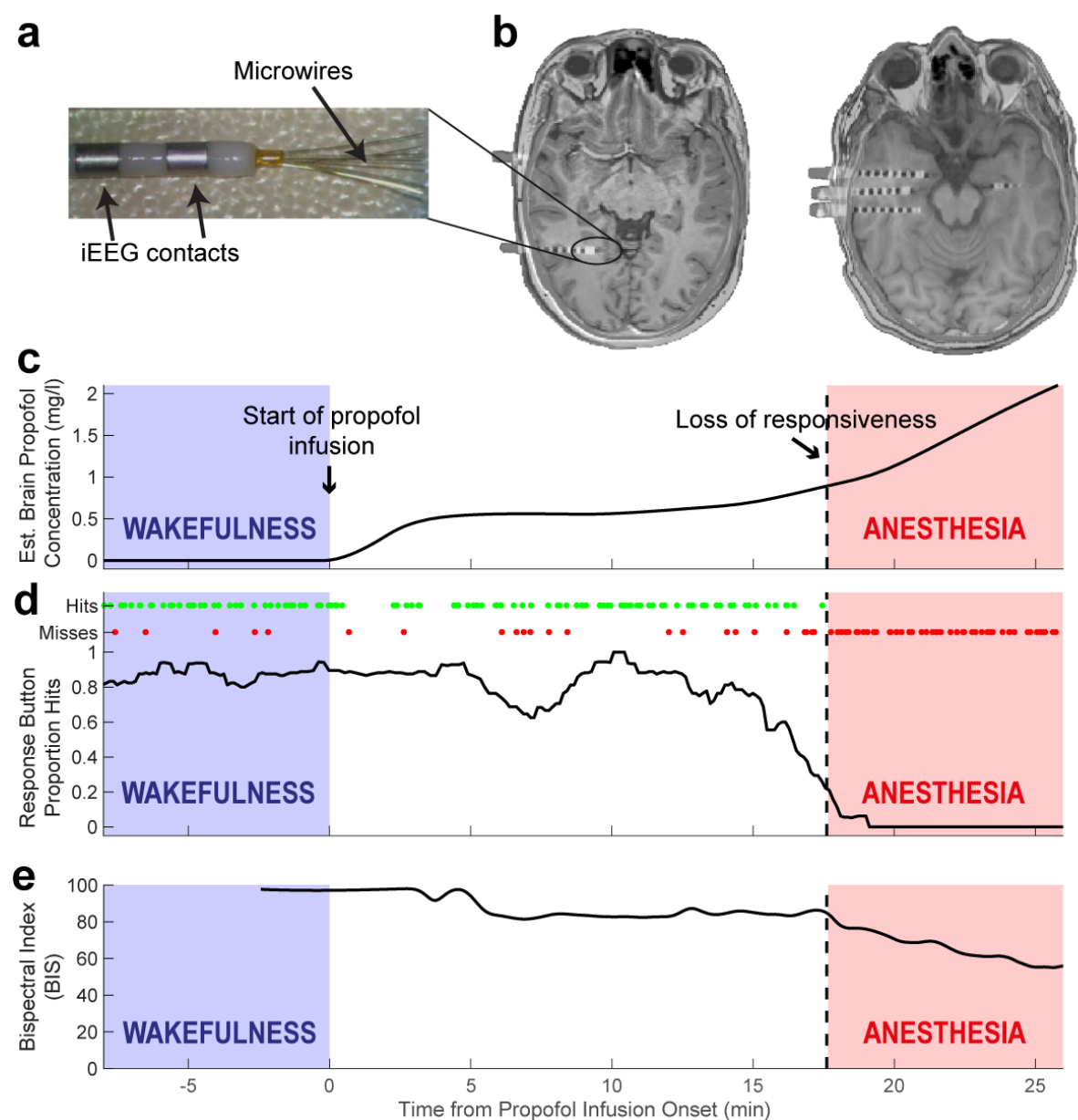
(a) Depth electrodes implanted in epilepsy patients for clinical monitoring, consisting of eight 1.5mm intracranial EEG (iEEG) contacts along the shaft, and eight 40µm microwires protruding from distal tip. (b) Representative pre-implant MRI co-registered with post-implant CT used to localize electrode positions. (c) Representative time-course of estimated

32

propofol concentration in brain tissue (y-axis) gradually increasing during experiment. Shaded

regions mark intervals of wakefulness (blue) and anesthesia (red) used for subsequent data

analysis. (d) Time-course of behavioral performance on the auditory task (individual task

hits/misses as green/red dots, plotted above averaged proportion of trials with hits). Vertical

dotted line, loss of responsiveness. (e) Bispectral index (BIS).

Figure 2. Anesthesia-induced LOC disrupts auditory responses in association cortices
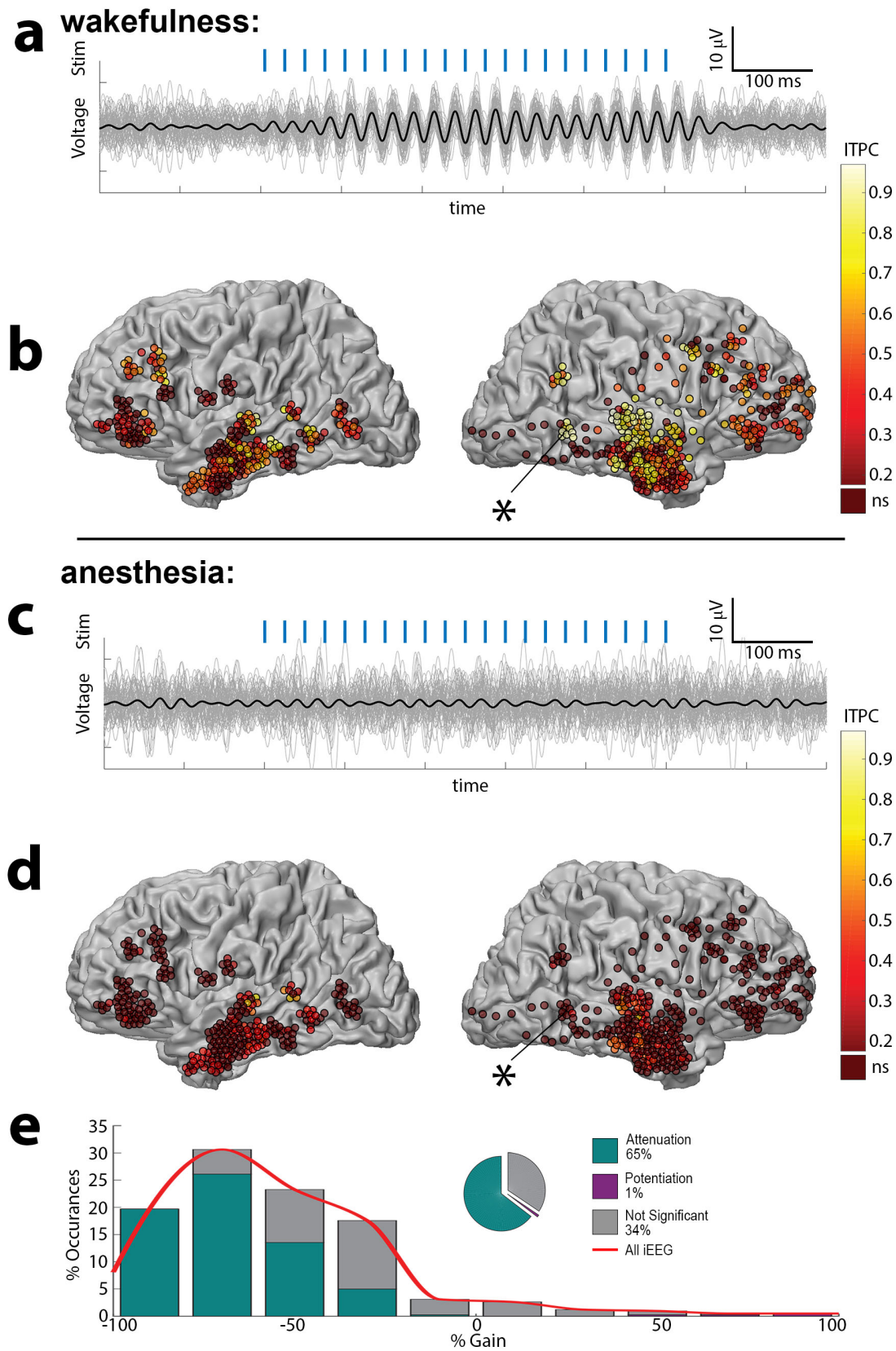
(a) Responses to 40Hz click-train (stimulus, in blue) in a representative iEEG electrode in the Superior Temporal Sulcus (asterisk) during wakefulness. Thick black trace marks the average response, while thin gray traces show individual trials (b) Inter Trial Phase Coherence at 40Hz (ITPC) for each iEEG electrode (n = 612 in 9 sessions) during wakefulness, as shown on a grey-white matter boundary surface as seen from lateral view. (c) Responses of the same iEEG electrode shown in (a) during anesthesia reveal disruption of reliable responses upon LOC. (d) ITPC of the same iEEG electrodes shown in (b) revealing disruption of responses outside the primary auditory cortex. (e) Quantification of the 424 iEEG contacts showing significant responses above baseline, reveal that 65% undergo significant attenuation under anesthesia, compared to only 1% showing potentiation. The red curve represents the smoothed histogram and is used for comparison in later figures.

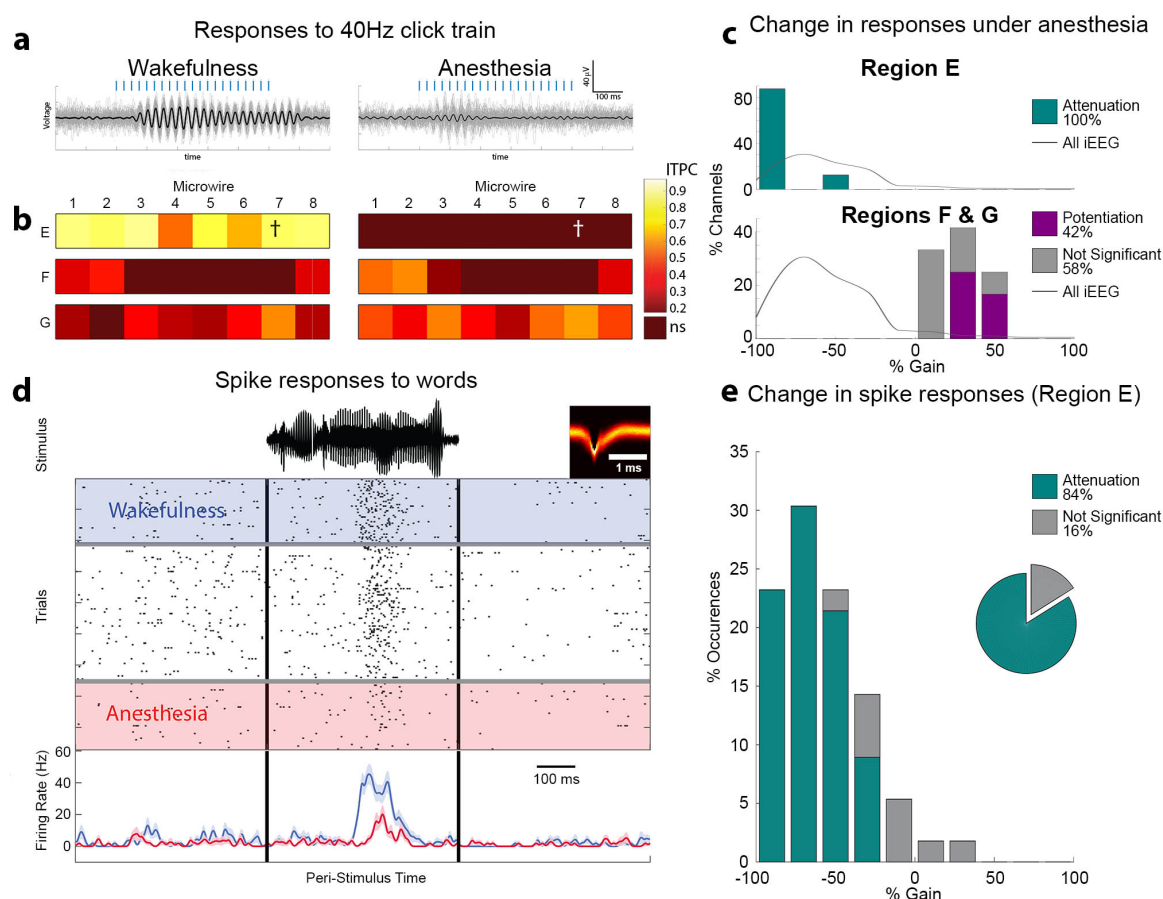**Figure 3. Significant responses in primary auditory cortex persist upon anesthesia-induced LOC**
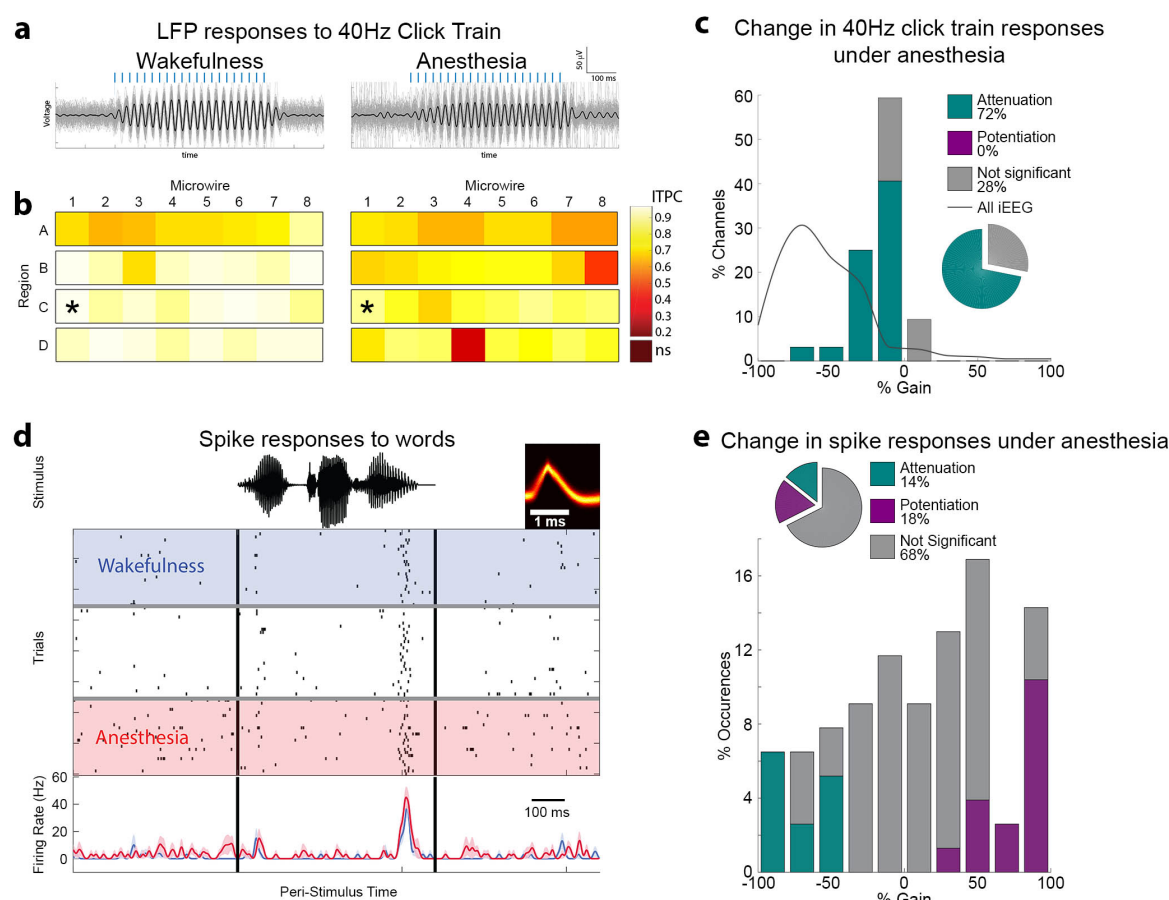
(a) Responses to 40Hz click-train in a representative PAC electrode during wakefulness (left) and anesthesia (right). Thick black traces marks the average responses, while thin gray traces show individual trials. (b) Responses (ITPC) to 40Hz click-trains across all PAC microwires (n = 32, regions A-D) during wakefulness (left) and anesthesia (right) reveals significant responses persisting upon anesthesia-induced LOC. Asterisks mark the specific microwire whose responses are shown above. (c) Histogram of gain in response under anesthesia for all 32 PAC microwires shows only minimal inhibition (bars), especially when compared to the marked inhibition seen across the brain in iEEG contacts (grey curve). (d) Raster plot and peri-stimulus time histogram (PSTH, below) of representative PAC neuronal

response to a word (stimulus waveform on top in black). Rows (top to bottom) mark

individual trials during deepening propofol anesthesia. Blue shading and time-course,

wakefulness; Red shading and time-course, anesthesia. (e) Quantitative analysis across all

PAC responses (n = 77 in 20 neurons) reveals that 68% of responses were not significantly

different between wakefulness and anesthesia, 14% were attenuated in anesthesia, and
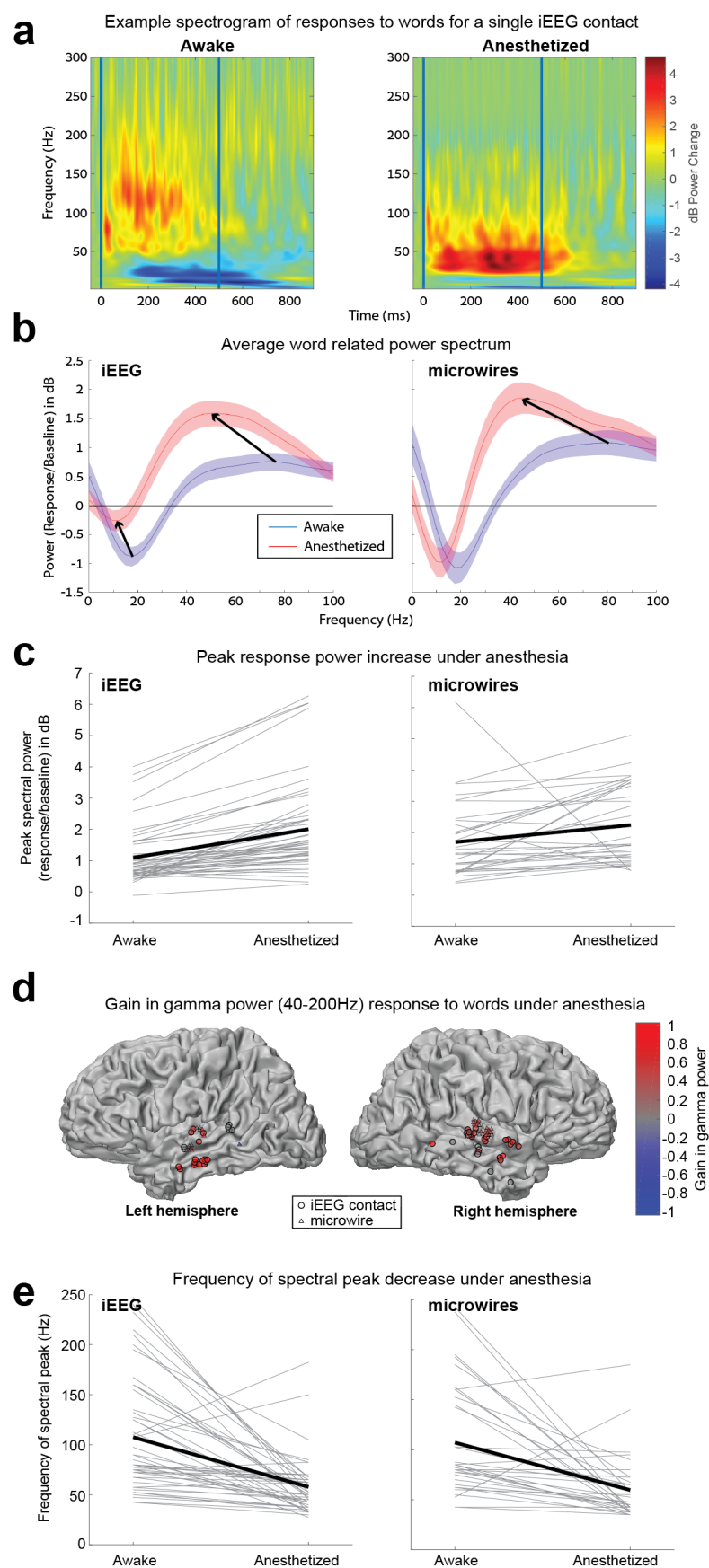
18% were potentiated in anesthesia.

Figure 4. High-order auditory responses upon anesthetic-LOC

(a) Responses to 40Hz click-train in a representative high-level auditory electrode during wakefulness (left) and anesthesia (right). Thick black traces marks the average responses, while thin gray traces show individual trials. (b) Responses (ITPC) to 40Hz click-trains across all high-level auditory microwires (n = 24, regions E,F,G) during wakefulness (left) and anesthesia (right). Cross marks the specific microwire whose responses are shown above, and from which the neuronal unit below (d) was recorded. Note attenuation to noise levels upon anesthesia-induced LOC in Region E, and weak potentiation of responses in Regions F & G. (c)

Histograms of gain in response under anesthesia for all 20 responding higher auditory microwires (Region E, top; and Regions F & G) showing variously mainly potentiation (purple) or attenuation (cyan bars) depending on the region. This is in contrast to the marked inhibition seen across the brain in iEEG contacts (grey curve). (d) Raster plot and peri-stimulus time histogram (PSTH, below) of representative higher auditory cortex (Region E) neuronal response to a word (stimulus waveform on top in black). Rows (top to bottom) mark individual trials during deepening propofol anesthesia. Blue shading and time-course, wakefulness; Red shading and time-course, anesthesia. (e) Quantitative analysis across all the high-level auditory responses from the same Region E (n = 56 in eight neurons) reveals that 84% of responses were significantly attenuated and none were significantly potentiated. Note that this attenuation is in line with the changes in ITPC to 40Hz from the same region shown above.

Figure 5. Induced gamma power responses to words upon anesthetic-LOC

a   Example spectrogram of responses to words for a single iEEG contact

b   Average word related power spectrum

c   Peak response power increase under anesthesia

d   Gain in gamma power (40-200Hz) response to words under anesthesia

e   Frequency of spectral peak decrease under anesthesia

(a) Example of a single temporal lobe iEEG contact event related spectral power (ERSP) averaged across words, demonstrating an increase in peak power, a reduction in the frequency of the power peak, and reduction in alpha/beta desynchronization, under anesthesia. (b) The power spectrum averaged over all 50 significantly responding (p<0.005) iEEG contacts (left) and all 34 significantly responding microwires (right), shows the same increase in peak power and shift to lower frequencies of the power peak. The iEEG spectrum also shows the reduction in alpha/beta desynchronization noted above. The peak power (c) and frequency of the power peak (d) plotted for each individual responding iEEG contact/microwire shows that these changes are consistent across contacts. (e) Plot of all 50 responding iEEG contacts and 34 responding microwires colored according to gain in gamma power under anesthesia. We see that responses are clustered exclusively around the temporal lobe, and in 83/84 case show increased power or no change.